



Promoting role of bismuth on carbon nanotube supported platinum catalysts in aqueous phase aerobic oxidation of benzyl alcohol



Chunmei Zhou^{a,b}, Zhen Guo^a, Yihu Dai^a, Xinli Jia^a, Hao Yu^{c,**}, Yanhui Yang^{a,*}

^a School of Chemical and Biomedical Engineering, Nanyang Technological University, Singapore 637459, Singapore

^b State Key laboratory of Silicon Materials, Department of Materials Science and Engineering, Zhejiang University, Hangzhou 310027, China

^c The School of Chemistry and Chemical Engineering, South China University of Technology, Guangzhou 510640, China

ARTICLE INFO

Article history:

Received 8 April 2015

Received in revised form 30 June 2015

Accepted 25 July 2015

Available online 29 July 2015

Keywords:

Platinum

Bismuth oxides

Benzyl alcohol

Aerobic oxidation

Synergic effect

ABSTRACT

PtBi/CNT catalyst was synthesized by a one-step polyol reduction method assisted by microwave radiation, and its catalytic performance was investigated in aerobic oxidation of benzyl alcohol in the aqueous phase. Pt and BiO_x species uniformly dispersed on the CNT surfaces and strong synergic interaction between them occurred, which confirmed by the comprehensive analysis of TEM, XRD, XPS and electrochemical characterizations. Further investigations revealed that the synergic effect effectively promoted the activation of both molecular oxygen and benzyl alcohol substrate; also protected Pt active sites from over-oxidation. The advantage of such synergic effect was reflected in the increased yield for the desired product benzaldehyde: PtBi/CNT catalyst exhibited about 3.5 times higher yield toward benzaldehyde compared to Pt/CNT catalyst. Furthermore, owing to the positive effect of Bi avoiding Pt from oxidizing, the deactivation of PtBi/CNT (with 2% selectivity and 9% conversion decrease) is much slower than that of Pt/CNT (with 8% selectivity and 39% conversion decrease) after six reaction cycles. PtBi/CNT catalyst was proved as a remarkably effective catalyst with high stability for the aerobic oxidation of benzyl alcohol.

© 2015 Elsevier B.V. All rights reserved.

1. Introduction

Bismuth as an excellent promoter of p-electron metal has attracted extensive attention in heterogeneous catalysis within both fundamental research and industrial applications. Significantly enhanced catalytic performance was obtained on Bi-promoted Pt- or Pd-based catalysts in the selective oxidation of alcohols with molecular oxygen as the oxidant in aqueous solutions [1–9]. In the early 1990s, Mallat et al. firstly reported the Bi-promoted carbon and alumina supported Pd catalysts with improved conversion and selectivity in the oxidation of 1-methoxy-2-propanol to 1-methoxy-2-propanone [10]. PtBi/C was later found with remarkably improved catalytic performance than Pt/C on selective oxidation of glycerol to dihydroxyacetone (DHA) by Kimura et al. [11,12] and Garcia et al. [13]. They revealed that with the same Pt loading (5% wt.), Pt/C yielded only 4% DHA at 37% glycerol conversion, and Pt-Bi/C yielded 20% DHA at 25% conversion; another co-impregnated PtBi/C catalyst yielded 37% DHA at 75% conversion. PdBi/C was also reported in the catalytic oxidation

of glucose to gluconate or gluconic acid by Besson et al. [14] and Wenkin et al. [15]. Since then, Bi-promoted Pt- and Pd-based catalysts have been employed in many other alcohol and aldehyde oxidation reactions, such as glyoxal [16], L-sorbose [17], 9-decen-1-ol [18], polyethylene glycol dodecyl ether [19], *n*-butanol [20] and so on.

In addition to the aforementioned straight chain alcohols and aldehydes, Baiker et al. [21–29] had made great effort on the selective oxidation of aromatic alcohols (such as cinnamyl alcohols, 1-phenylethanol and benzyl alcohol) on alumina, carbon or polyaniline-supported Pd-Bi and Pt-Bi catalysts. Among these reactions, selective oxidation of benzyl alcohol to benzaldehyde is of importance because the product serves as the versatile intermediates in synthetic chemical industries [30]. More than 40 times higher conversion was achieved by modifying a 5% wt. Pt/Al₂O₃ catalyst with Bi (0.9% wt.) in the aerobic oxidation of benzyl alcohol when using either cyclohexane or toluene as the solvent [29].

The origin of the promoting role of Bi on Pd and Pt catalysts still remains unclear. Many early studies have proved that bismuth and lead as p-electron metals favored the oxidation of polyhydroxy carboxylic acids into their α -keto derivatives, which explained the promoting role of Bi on selectivity [11–13,31–33]. Presently, Bi was also shown to enhance selectivity in alcohol oxidation by suppressing parallel reaction on a Bi-modified AuPd/AC catalyst [34].

* Corresponding author. Fax: +86 65 67947553.

** Corresponding author. Fax: +86 20 8711 4916.

E-mail addresses: yuhao@scut.edu.cn (H. Yu), yhyang@ntu.edu.sg (Y. Yang).

The promoting effect of Bi on reaction rate [1,21,35] was referring to: (1) Bi formed a geometric blocking on noble metal, which decreased the size of active site ensembles and suppressed the strong adsorption of poisoning intermediates [36]. (2) OH_{ads} adsorbed on Bi adatoms to form new active sites, such as Pt-Bi- OH_{ads} [36]. (3) Bi promoters inhibited the corrosion of noble metal catalysts [37]. (4) High affinity of Bi for oxygen prevented noble metal from over-oxidation, and maintained its metallic state [14]. (5) Bi promoters and substrate materials can form complexes with chelating properties, enhancing the stability and activity of the catalyst [38,39]. In view of these mechanistic understandings, most studies about Bi-promoted Pt- or Pd-based catalysts focused on the following aspects: the synergic effect between Bi and the noble metals and the substrate materials [10,27,40–42]; the state of Bi on the catalysts, including Bi's content, valence state and contact mode with noble metals, which may be changed significantly due to different Bi precursor or preparation methods [15,16,35]; the adsorption modes of reactants, intermediates and products [24–26,29]; and the deactivation mechanism [43,44].

In this work, Bi-promoted Pt catalysts supported on carbon nanotube were synthesized by a microwave-assisted polyol reduction method. The synergic effect between Bi and Pt was discussed. The promoted effects of Bi as well as the optimization of catalyst and reaction conditions on aqueous phase aerobic oxidation of benzyl alcohol were investigated.

2. Experimental

2.1. Materials and catalyst synthesis

HNO_3 (69%), HCl (36%), H_2SO_4 (98%), KOH (99.9%), H_2PtCl_4 ($\text{Pt} \geq 37\%$ wt.), $\text{Bi}_2(\text{CO}_3)_2\text{O}_2$, benzyl alcohol (98%), benzaldehyde (98%), benzalacide (98%), ethylene glycol (EG), toluene (99.9%), and cyclohexane (99.9%) were obtained from Sigma-Aldrich. CNT was provided by Cnano Technology Ltd (with 97.1% purity, $241 \text{ m}^2/\text{g}$ S_{BET} and $0.05 \text{ g}/\text{cm}^3$ bulk density). The pristine CNT was pre-treated with concentrated HNO_3 at 413 K for 2 h to remove the impurities and to introduce surface oxygen-containing groups to enhance the metal dispersion [45]. The catalysts were prepared as following steps:

(1) Synthesis of CNT supported Bi or Pt catalysts:

The treated CNT (0.2 g) was suspended in 2 ml of DI water under ultra-sonication. Stoichiometric amount of $\text{Bi}_2(\text{CO}_3)_2\text{O}_2$ was dissolved to 1 M HCl aqueous solution to form Bi precursor salt solution (0.01 M). A volume of 1.3 mL of Bi precursor salt solution or a volume of 0.7 ml of 0.05 M H_2PtCl_4 aqueous solution was firstly added into above CNT aqueous solution, and then mixed sufficiently under ultra-sonication; the slurry was finally dried at 373 K in vacuum oven overnight. The as obtained compound of metal salt and CNT compounds were reduced by a polyol reduction method assisted under microwave radiation [46]. Typically, an amount of 0.1 g of such compound was dispersed in EG (40 ml) followed by sonicating for 10 min and placed in the microwave reactor (Sineo, MAS-II). The mixture was heated to 438 K in 0.5 min and kept at the same temperature for 1.5 min. The powder was filtrated and washed with DI water, and dried at 373 K in a vacuum oven. The as obtained samples were labeled as Bi/CNT and Pt/CNT. The Bi loading is 0.98% wt. for Bi/CNT and Pt loading is 4.95% wt. for Pt/CNT confirmed by ICP measurement.

(2) Synthesis CNT supported Pt and Bi catalysts:

PtBi catalysts were also prepared by the one-step microwave-assisted polyol reduction method. A volume of 722 μl of 0.05 M H_2PtCl_4 solution and stoichiometric amount of Bi precursor salt

solution were simultaneously added on 0.1 g of CNT, and followed by the microwave reduction. The obtained catalysts were denoted as PtBi/CNT. Their Pt contents maintain about 5% wt. while Bi/Pt molar ratios are controlled from 0.01 to 2.5, and if not differently indicated, the Pt/Bi molar ratio for PtBi/CNT equal 1. For comparison, Pt and Bi were also successively loaded to CNT by a two-step microwave reduction. Based on the loading sequence, the as obtain samples were donated as Pt-Bi/CNT (with Bi first loaded) and Bi-Pt/CNT (with Pt first loaded). All the metal contents and ratios of the obtained catalysts were confirmed by ICP and listed in Table S1.

2.2. Characterizations

Metal loadings for all the prepared catalysts were quantified via measuring the metal concentrations in dissolved solution of samples with 40% hydrofluoric acid, using inductively coupled plasma measurements (ICP, AA6800, Shimadzu). Transmission electron microscopy (TEM) images of metal catalyst nanoparticles were observed on the Philips TecnaiG² F20 operated at 200 kV. Scanning transmission electron microscopy-energy-dispersive X-ray spectroscopy (STEM-EDX) was carried out on the same equipment with a Sirion 200 field emission scanning electron microscope, following the same sample preparation procedure as described above. X-ray diffraction (XRD) patterns were recorded on the Bruker AXS D8 Focus diffractometer using a Ni filtered $\text{Cu K}\alpha$ radiation ($k = 0.154 \text{ nm}$), operated at 40 kV and 40 mA. Diffraction data were collected with a resolution of 0.02 degree (2θ). The valences of metals were analyzed by X-ray photoelectron spectroscopy (XPS, VG Escalab 250 spectrometer) equipped with an Al anode (Al $K\alpha = 1486.6 \text{ eV}$). The background pressure in the analysis chamber was lower than $1 \times 10^{-7} \text{ Pa}$. Measurements were conducted under 20 eV of pass energy, 0.1 eV of step, and 0.15 min of dwelling time. The binding energies (BEs) were corrected by the C_{1s} peaks of adventitious C at 284.6 eV. The curve fitting was carried out with a Gaussian–Lorentzian shape function to execute the convolution of the overlapped peaks.

The electrochemical characteristics were tested by voltammetries on an Autolab PGSTAT302 potentiostat operated at room temperature using a rotating disk electrode system. The cyclic voltammetry potentiodynamic polarization curves were recorded in 0.1 M KOH solution purged by nitrogen, and the scan rate was 50 mV/s. Oxygen reduction was measured in oxygen saturated 0.1 M KOH solution by liner potential sweep at 10 mV/s. Electro-oxidation of benzyl alcohol was measured in 0.2 M benzyl alcohol using 0.1 M KOH as electrolyte.

2.3. Catalytic reaction

The benzyl alcohol aerobic oxidation was carried out in a batch reactor under atmospheric conditions. A certain amount of substrates, solvents and catalysts were added into a flask and stirred at 1200 rpm by a magnetic stirrer and heated to 348 K in the oil bath. The vapor products were condensed by a reflux condenser. Oxygen (25 mL/min) was controlled and bubbled into the mixture to initiate the reaction. After the reaction, the catalyst powder was filtered prior to the analysis of filtrate. And for the recycling test, the used catalyst powder was washed successively with 1 M NaOH aqueous solution, water and acetone, and finally dried over night in vacuo under 343 K before reusing. The reactant and product were analyzed by an Agilent gas chromatograph 6890 with a HP-5 capillary column (0.32 mm I.D. \times 30 m, packed with silica-based Supelcosil), and flame ionization detector (FID).

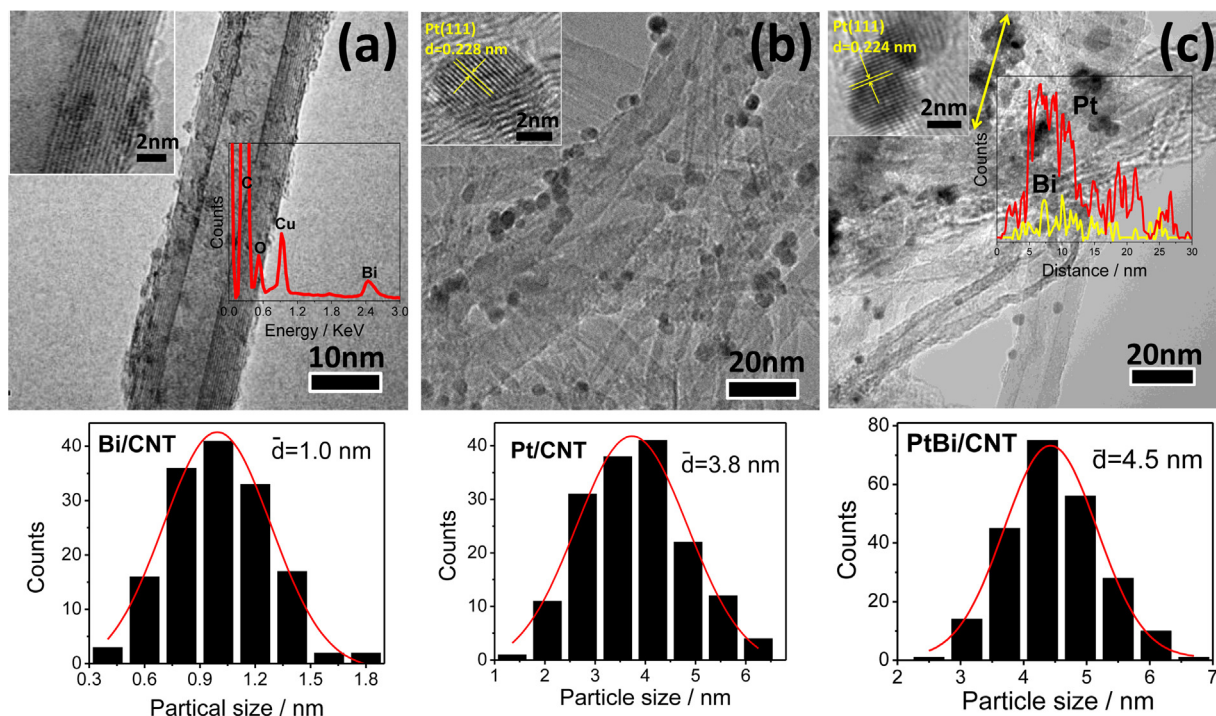


Fig. 1. TEM images, particle size distribution and EDS spectra of Bi/CNT (a), Pt/CNT (b) and PtBi/CNT (c).

3. Results and discussion

3.1. Characterizations of CNT supported Bi, Pt and PtBi samples

The morphology and distribution of Pt and Bi species on the surface of CNT were observed by TEM images and EDX spectra. For Bi/CNT, as shown in Fig. 1a, nanoparticles (with 1 nm average diameter) dispersed uniformly on CNT surface. Clear Bi elemental peaks appeared on EDX spectrum (inset of Fig. 1a right) of the representative areas, which demonstrates that those nanoparticles are Bi species. However, no obvious lattice fringe was found from its high resolution (HR) TEM image (inset of Fig. 1a top left), and Bi lattice peaks were also absent in the XRD pattern (Fig. 2) of Bi/CNT, which indicates that Bi species were uniformly dispersed as tiny grains and with low crystallinity degree. As for

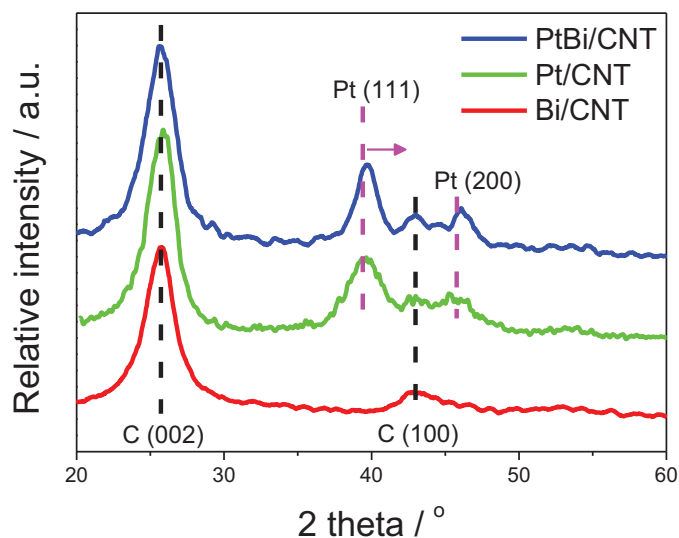


Fig. 2. XRD patterns of Bi/CNT, Pt/CNT and PtBi/CNT.

Pt/CNT (Fig. 1b), Pt nanoparticles were observed uniformly dispersed on CNT surfaces, with 3.8 nm average diameter. According to its HR-TEM image (Fig. 1b inset), the distance between two Pt(111) lattice planes is around 0.228 nm, which is consistent with the XRD results (Fig. 2), for which the Pt(111) peak is located at 39.5° of 2θ (JCPDS#04-0802). As for PtBi/CNT (Fig. 1c), larger nanoparticles (with 4.5 nm average diameter) were observed uniformly dispersed on CNT surface. The EDX profiles of Pt L α and Bi L α X-rays are plotted along the line of a cluster of representative nanoparticles (inset of Fig. 1c right); both Pt and Bi are detected, confirming the successful preparation of Pt and Bi closely contacted nanoparticles. To further observe its HR-TEM images (inset of Fig. 1c top left), the distances between two Pt (111) lattice planes are found distinctly shrank to approximately 0.224 nm. It suggests that some Bi atoms were doped into Pt's lattice space, which indicates strong synergic effect would exist between Pt and Bi in PtBi/CNT catalyst. Separated Bi species were hardly observed by HR-TEM, and Bi lattice peaks were still absent in XRD pattern of PtBi/CNT (in Fig. 2). Huang et al., reported their approach using microwave to synthesize Bi-modified Pt nanoparticle catalysts, Bi species were hardly observed by XRD and TEM when Bi was uniformly dispersed and with its loading lower than 10% wt. [47]. It indicates that Bi species were uniformly dispersed in PtBi/CNT in common with Bi/CNT. However, Pt XRD peaks of PtBi/CNT emerge obvious difference compared to that of Pt/CNT. The Pt (111) diffraction peak of PtBi/CNT is sharper and the position right shifts about 0.1 degrees compared to that of Pt/CNT. The particle sizes calculated using Pt (111) diffraction peak are 3.8 and 4.3 nm for Pt/CNT and PtBi/CNT, respectively; which is well according with the results of TEM particle size statistics (Fig. 1). And the slightly left shift of Pt (111) XRD peak is also well consistent with the crystal spacing shrinking of Pt (111) of PtBi/CNT observed from HR-TEM (inset of Fig. 1c top left), which all indicated that Bi atoms may alloy with Pt to change the crystal lattice of Pt [32,33]. Both XRD and TEM results reveal that Pt and Bi particles can be dispersed uniformly on CNT surfaces by the microwave-assisted polyol reduction method, and Pt and Bi has well contact and strong synergic effect with each other in PtBi/CNT.

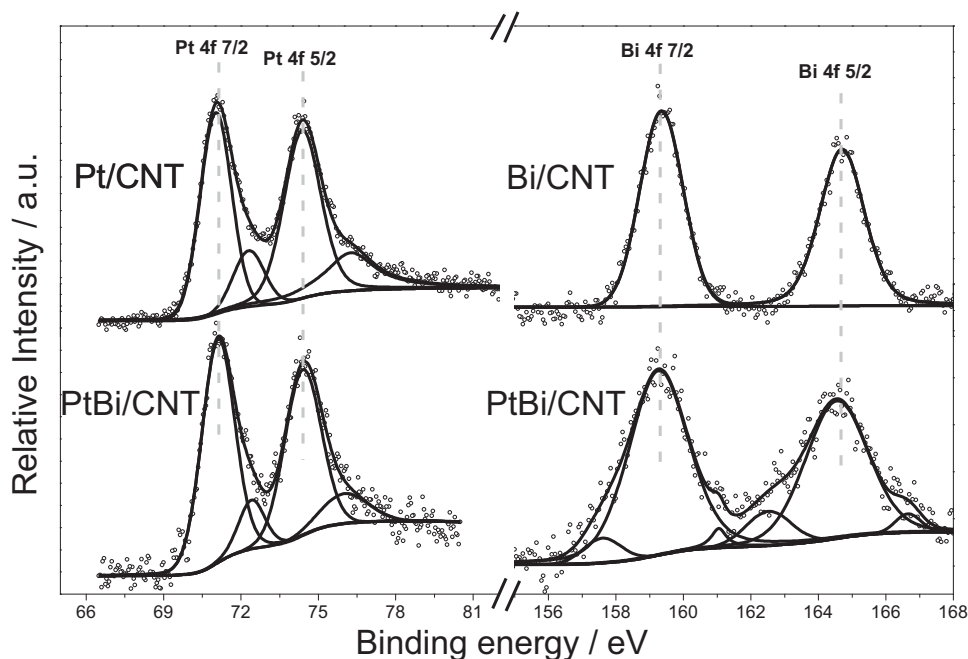


Fig. 3. XPS spectra of Bi/CNT, Pt/CNT and PtBi/CNT.

XPS spectra (Fig. 3) were further used to describe the electronic effect for Pt and Bi in Bi/CNT, Pt/CNT and PtBi/CNT, and relative result data are also listed in Table 1. The Pt 4f spectrum for Pt/CNT is described by two Gaussian doublets, one located at 71.0 eV (Pt 4f_{7/2}) and 74.4 eV (Pt 4f_{5/2}), which is the characteristic feature of metallic Pt; and another weaker doublets at 72.2 and 76.2 eV can be assigned to platinum oxide [48]. Calculated by the peak area, the content of PtO is about 23.3%. The Pt 4f spectrum of PtBi/CNT can also be correspondingly described by two pair of peaks. Compared to Pt/CNT, its binding energies and the content of PtO have negligible changes, indicating that Pt valence status has slight difference between Pt/CNT and PtBi/CNT. The Bi 4f spectrum for Bi/CNT can be described by a pair of peaks at 159.4 eV (Bi 4f_{7/2}) and 164.7 eV (Bi 4f_{5/2}), which are typical characteristic peaks of Bi₂O₃ [49,50]. While

for PtBi/CNT, the Bi 4f_{7/2} and Bi 4f_{5/2} signals with much larger peak width than that of Bi/CNT, should be described by 3 pairs of peaks. One pair of the strongest peaks at 159.2 and 164.5 eV is assigned to Bi₂O₃, and accounts for 84.1% of the total Bi amount; another weaker pair of peaks at 157.6 and 162.5 eV is assigned to Bi metal [49,50], and accounts for 10.2%; the other pair of peaks at 161.0 and 166.7 eV is assigned to Bi oxides with higher value status than Bi₂O₃, denoted as Bi₂O_{3+x} in Table 1b, and which accounts for 3.7%. To summarize these XPS results, the main existing status of Pt component in both of Pt/CNT and PtBi/CNT is Pt⁰; and almost all of Bi component in Bi/CNT is Bi₂O₃; and dissimilarly, most Bi component in PtBi/CNT is Bi₂O₃ excepting 10.4% of Bi⁰ and 3.7% Bi₂O_{3+x} species. Obviously, with similar preparation conditions, the valence status of Bi in Bi/CNT is quite different with in PtBi/CNT, which should be ascribed by the electronic synergic effect of Pt. The electronic status difference is according with the structure variance observed by HR-TEM and XRD for these catalysts, and further confirms that strong synergic effect between Pt and Bi exists in PtBi/CNT catalysts.

Cyclic voltammetry can be used to precisely analyze the surface properties of metal catalysts. Fig. 4a presents the cyclic voltammograms of CNT and Pt/CNT modified glassy carbon electrodes. At about −0.37 V, the −OH chemisorption starts on Pt/CNT. Then the Pt–O forms at about −0.15 V. After the reversion of potential, the Pt–O and oxygen molecules near the surface are reduced from about −0.2 V and peaked at −0.3 V. The hydrogen adsorption on Pt sites starts at about −0.58 V to form Pt–H. After scan reversion, H₂ molecules near the electrode and the Pt–H are oxidized. [51,52] For concision, only voltammetric curves with potential range from −0.95 to 0.25 V were compared in Fig. 4b. For Bi/CNT, one oxidation peak emerges at −0.52 V with the onset oxidation potential of −0.66 V. As to PtBi/CNT, the hydrogen adsorption and desorption peaks of Pt are disappeared, which indicates that the hydrogen adsorption and desorption behavior of Pt is suppressed by doping with Bi species. Similar results were also reported by other researchers [9,53]. Alternatively, a pair of overlapping peaks appear at the range from −0.5 to 0.1 V of PtBi/CNT curves, which are attributed to the oxidation of Pt and Bi species. The left broad peak can be ascribed to the oxidation of Bi or BiO_x [47,54–56], with higher peak potential (near −0.3 V) and onset potential (near

Table 1
XPS data of different samples for Pt 4f (a) and Bi 4f (b).

(a) Pt 4f				
Catalysts	Species	Peak position/eV	Content/%	
		Pt 4f 7/2	Pt 4f 5/2	
Pt/CNT	Pt ⁰	71.0	74.4	76.7
	PtO	72.2	76.2	23.3
PtBi/CNT	Pt ⁰	71.0	74.4	77.5
	PtO	72.1	76.1	22.5
Pt/CNT (used)	Pt ⁰	71.1	74.5	71.1
	PtO	72.4	76.4	28.9
PtBi/CNT (used)	Pt ⁰	71.0	74.4	78.0
	PtO	72.1	76.1	22.0
(a) Bi 4f				
Catalysts	Species	Peak position/eV	Content/%	
		Bi 4f 7/2	Bi 4f 5/2	
Bi/CNT	Bi ₂ O ₃	159.4	164.7	100
PtBi/CNT	Bi ₂ O ₃	159.2	164.5	84.1
	Bi ⁰	157.6	162.5	10.2
PtBi/CNT (used)	Bi ₂ O _{3+x}	161.0	166.7	3.7
	Bi ₂ O ₃	159.3	164.6	79.3
	Bi ⁰	157.6	162.6	7.6
	Bi ₂ O _{3+x}	160.9	166.6	13.1

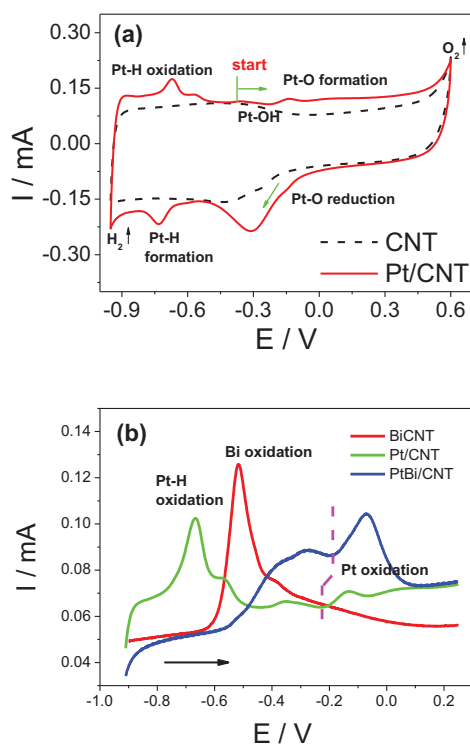


Fig. 4. Cyclic voltammograms for CNT and Pt/CNT modified GC electrodes (a) potentiodynamic current curves for -0.95 to 0.2 V for Bi/CNT, Pt/CNT and PtBi/CNT (b) (conditions: in 0.1 M KOH, with N_2 saturated, potential scan rate = 50 mV/s).

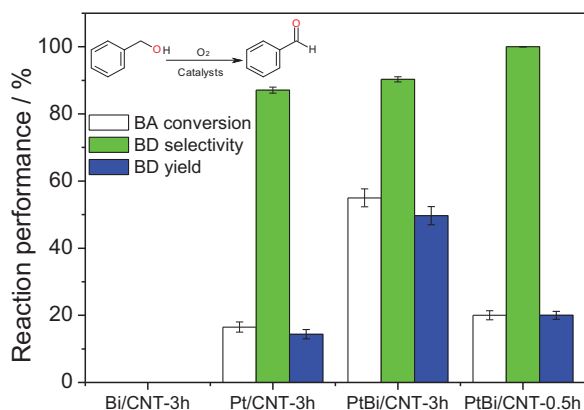


Fig. 5. Conversion, selectivity and yield of benzaldehyde (BD) of different catalysts in the aerobic oxidation of benzyl alcohol (BA) (conditions: benzyl alcohol 3 mmol, deionized water 15 mL, catalyst 12 mg (0.6 μ mol Bi, 3 μ mol Pt), 348 K, 3 h, O_2 flow rate 25 mL/min, carbon balance $>99.5\%$).

-0.6 V) than that of Bi/CNT. The right peak can be ascribed to the oxidation of Pt to PtO, also with higher peak potential (near -0.1 V) and onset potential (near -0.2 V) than that of Pt/CNT. Evidently, the variation of onset and peak potentials for PtBi/CNT is due to the strong synergic effect of Pt and Bi. Based on the comparison of all these oxidation peak potentials for different catalysts, the difficulty sequence for oxidation of each species can be assumed to: Pt in PtBi/CNT $>$ Pt in Pt/CNT $>$ Bi in PtBi/CNT $>$ Bi in Bi/CNT, and the synergic effect of Bi apparently increased the difficulty of Pt's electro-oxidation.

3.2. Catalytic performance of the catalysts

Fig. 5 shows the conversion, selectivity and benzaldehyde yield for the aqueous aerobic oxidation of benzyl alcohol over Bi/CNT,

Pt/CNT and PtBi/CNT catalysts. Firstly, there is no conversion when using Bi/CNT as catalyst, indicating that Bi species has no catalytic activity in this reaction. Pt/CNT presents 16.5% conversion and 87.1% selectivity of benzaldehyde, while PtBi/CNT presents 55% conversion and 90.3% selectivity of benzaldehyde. With the same amount of Pt, the benzaldehyde yield for PtBi/CNT is 3.5 times as that of Pt/CNT. For comparing the selectivity at similar conversions (near 20%), the performance of PtBi/CNT with shorter reaction time (0.5 h) was also recorded, PtBi/CNT presents 100% selectivity of benzaldehyde, obviously exceeds that of Pt/CNT (87.1%). Distinctly, PtBi/CNT presents much higher activity and benzaldehyde selectivity than Pt/CNT.

The activation of benzyl alcohol and oxygen was investigated by electrochemical measurements. The aerobic oxidation can be regarded as two half reactions: alcohol electro-oxidation and oxygen electro-reduction [57,58]. The oxygen activation of different samples is firstly analyzed by the electro-reduction of oxygen and presented in Fig. 6a. CNT shows poor activity for oxygen reduction; the onset potential is at about -0.22 V and max reduction current -0.3 mA. After loading Bi species onto CNT, the oxygen reduction activity is promoted, showing about 0.05 V lower (right-shift) onset potential compared to CNT, and the highest reduction current is about -0.4 mA for Bi/CNT. As to Pt-containing samples, the oxygen reduction onset potentials are about -0.22 and -0.19 V, and the max reduction currents are -0.45 and -0.64 mA for Pt/CNT and PtBi/CNT respectively. The adding of Bi depresses the onset potentials and increases the current, which indicates that Bi species can obviously enhance the activation of oxygen.

The alcohol activation over different samples are analyzed by the electro-oxidation of benzyl alcohol and shown in Fig. 6b. For Bi/CNT, no alcohol oxidation signal can be detected. For Pt/CNT, two obvious oxidation peaks are observed. Based on our previous results [57], the first peak (-0.1 V) is due to the benzyl alcohol oxidation to benzaldehyde, and the second peak (0.25 V) is ascribed to the benzaldehyde oxidation to benzoic acid. For PtBi/CNT catalyst, only the first oxidation peak was observed, while the second peak was severely suppressed. Similar electro-oxidation of benzaldehyde was also conducted using Pt/CNT and PtBi/CNT as catalysts (for concision, the voltammetry potentiodynamic polarization curves were shown in Supporting information Fig. S1), only the second peak appeared on Pt/CNT, and no oxidation peak appeared on PtBi/CNT. The suppression of second peak demonstrates Bi species suppressing the oxidation of benzaldehyde to benzoic acid, which is well interpreted the high benzaldehyde selectivity of PtBi/CNT. Meanwhile, the max peak current for PtBi/CNT is 5 times higher than that of Pt/CNT, which indicates Bi species can remarkably enhance the activation of benzyl alcohol.

From electrochemical measurements, it was probed that Pt is the active site for activation of benzyl alcohol and oxygen, while Bi itself can not activate benzyl alcohol. However, Bi presents well performance on oxygen activation and remarkably promotes the activation of benzyl alcohol by synergic effect with Pt. To verify the roles of each component, XPS spectra of Pt/CNT and PtBi/CNT after 3 h aerobic oxidation of benzyl alcohol were also analyzed (for concision, XPS spectra of the catalysts before and after reaction were shown in Supporting information Fig. S2, and their relative result data are also listed in Table 1). As shown in Table 1a, compared to fresh Pt/CNT, the PtO content of Pt/CNT-used (calculated by the Pt 4f_{7/2} and Pt 4f_{5/2} peaks) is increased from 23.3% to 28.9% , which indicated that part of Pt in the Pt/CNT may be oxidized by oxygen during the reaction. However, no remarkable change is observed for Pt 4f XPS spectra of PtBi/CNT before and after the aerobic oxidation reaction. From the data of Bi 4f XPS spectra, comparing the spent PtBi/CNT catalyst to the fresh one, the content of metallic Bi (calculated by doublets of Bi 4f_{7/2} and Bi 4f_{5/2}) is decreased from 10.2% to 7.6% (as shown in Table 1b), which indicates that

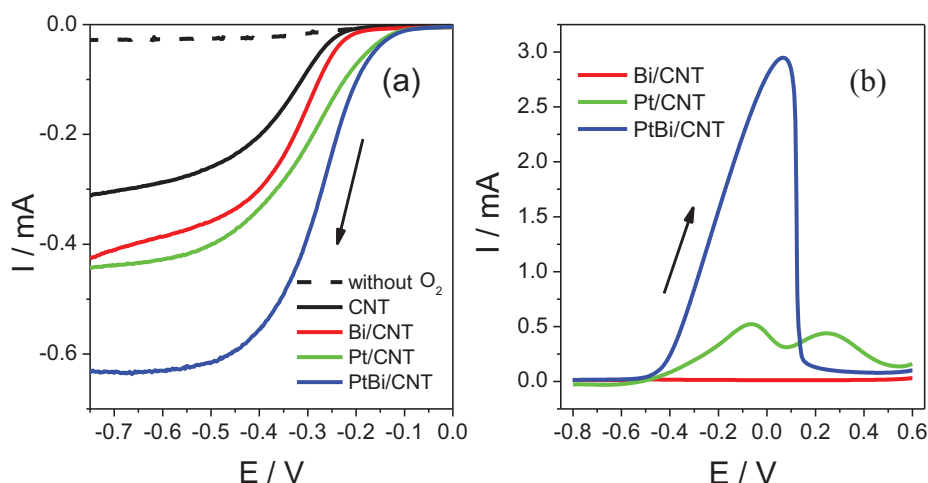


Fig. 6. Potentiodynamic current curves of oxygen electro-reduction (a) and benzyl alcohol electro-oxidation (b) on different catalysts modified glass carbon electrodes (conditions: (a) in 0.1 M KOH, with O₂ saturated, potential scan rate = 10 mV/s, under rotating condition at 2000 rpm; (b) in 0.2 M benzyl alcohol + 0.1 M KOH, with N₂ saturated, potential scan rate = 50 mV/s).

part of Bi species instead of Pt in PtBi/CNT are oxidized during the reaction, similar result was also reported on the AuBi catalyst [41], which is according with the redox status of the catalysts detected by electrochemical method (Fig. 4) that the synergic effect of Bi increased the difficulty of Pt's oxidation. It will protect the Pt active sites and promote the stability of the catalyst. Recycling catalytic experiments were conducted to test the stability of PtBi/CNT and Pt/CNT. As shown in Fig. 7, after 6 times recycle runs, Pt/CNT maintains 61% conversion and 92% selectivity as to the fresh one, while the PtBi/CNT maintain 91% conversion and 98% selectivity as to the fresh one. Generally, several reasons are ascribed to be responsible for the deactivation of Pt-based catalysts on aerobic oxidation of alcohols, including the aggregation or growing up of Pt particles, the oxidation of Pt and the corrosion losing of Pt by some acid products. [43,44] No obvious aggregation or growing up of Pt particles were observed on the TEM images of the reused Pt/CNT and PtBi/CNT catalysts (as shown in Fig. S3 a and b). Slightly leaching

of Pt was detected on both Pt/CNT and PtBi/CNT catalysts. After 6 times cycling, about 1 wt.% Pt of the Pt/CNT and about 1 wt.% Pt and 2 wt.% Bi of the PtBi/CNT were dissolved into the collected solutions (detected by ICP). Obviously, PtBi/CNT presents better stability than Pt/CNT, which mainly due to the protection effect of Bi which avoiding Pt's oxidation. And the continuous slow deactivation of PtBi/CNT may be due to the corrosion losing of Pt and Bi.

Based on above evidences, the mechanism of benzyl alcohol aerobic oxidation over Pt/CNT and PtBi/CNT is illustrated in Scheme 1 and demonstrated as the following Eqs. from (a1) to (b4).

For Pt/CNT catalyst:

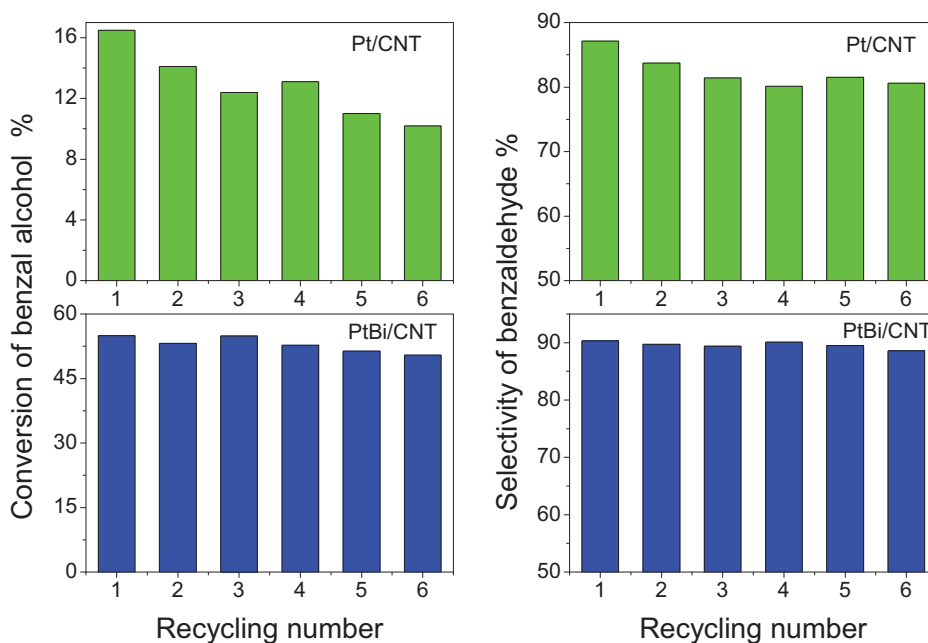
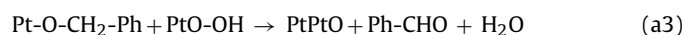
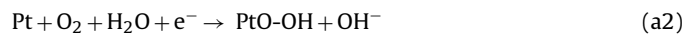
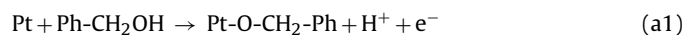
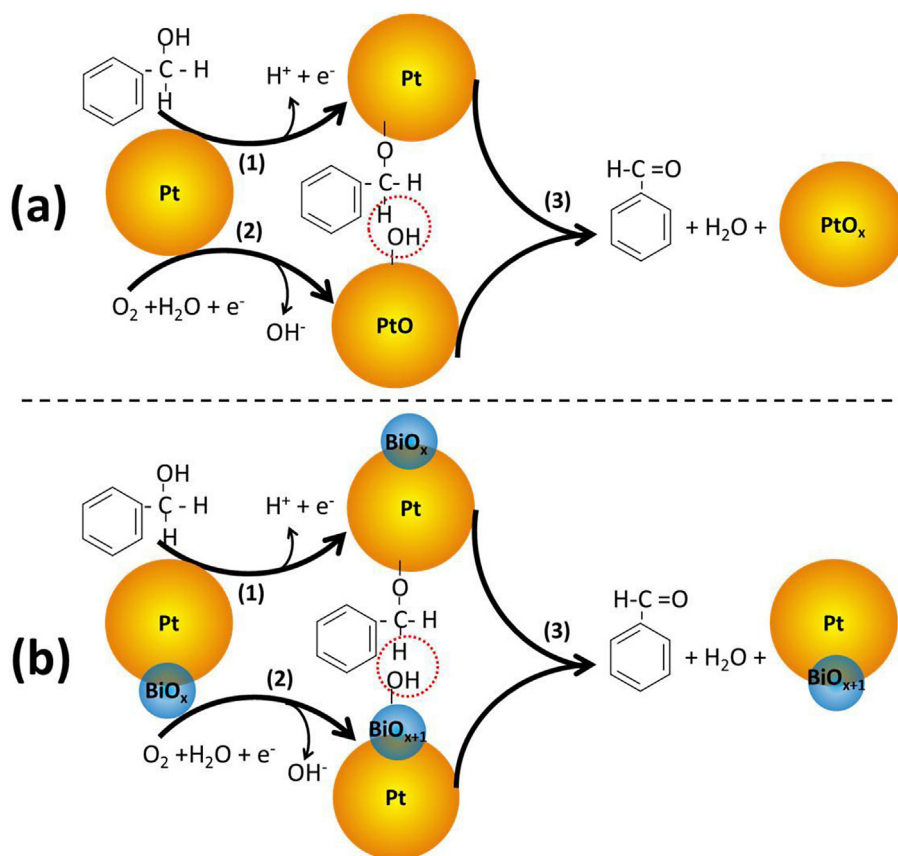
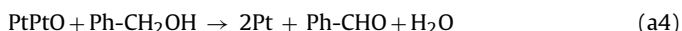


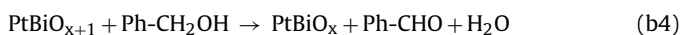
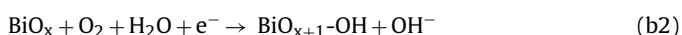
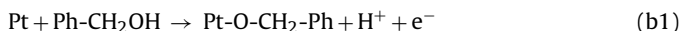
Fig. 7. Recycle conversions and selectivities for Pt/CNT and PtBi/CNT in aerobic oxidation of benzyl alcohol (conditions: benzyl alcohol 3 mmol, deionized water 15 mL, 348 K, 3 h, O₂ flow rate 25 mL/min, carbon balance > 99.5%).



Scheme 1. Reaction scheme for the selective oxidation of benzyl alcohol to benzaldehyde over Pt (a) and PtBi (b) catalyst.



For PtBi/CNT catalyst (the initial Bi species denoted as BiO_x):



The catalytic cycle proceeded in four steps. For Pt/CNT catalysts, benzyl alcohol adsorption on Pt occurs, and the alcohol is reduced by Pt to form Pt-alcoholate (a1). Then Pt further activates the oxygen to form -OH_{ads} species, while at the same time part of Pt metal will also be oxidized by molecular oxygen, resulting PtO- OH_{ads} species (a2). Then, dissociated hydrogen is removed by -OH_{ads} species from α -C of benzyl alcohol and benzaldehyde, Pt and PtO sites are released (a3). Most PtO sites will continue react and be reduced by the hydroxyl of benzyl alcohol to release Pt metal sites again and complete the cycle (a4). However, the formation of PtO in step (a2 and a3) would block some of the active Pt metal site and remarkably lower the entire reaction rate. On the other hand, over PtBi/CNT catalyst, the introduced interface of Pt and BiO_x (or Bi) species is active to molecular oxygen, and Bi or BiO_x species are easily oxidized by the surplus oxygen, which can protect the Pt active site from being oxidized. Thus the strong interaction of BiO_x /Pt can not only promote the activation of molecular oxygen, but also prevent the formation of PtO species blocking the passway of alcohol activation on Pt sites, which indirectly promotes the alcohol activation and further oxidation. BiO_x species can also be reduced by further reacting with benzyl alcohol, to perform the catalytic cycle, while has no influence on the alcohol oxidation on Pt sites. Therefore, PtBi/CNT with interface of Pt and Bi species provides good

activity and stability in aerobic oxidation of benzyl alcohol, and the electro-oxidation test also confirmed it achieves high selectivity by suppressing the formation of by-products.

3.3. Optimizing conditions for PtBi/CNT in the selective oxidation reactions

For exploring best performance of PtBi catalysts, further optimization of reaction condition was carried out. The effect of Pt and Bi loading sequence and Bi content were first investigated. Similar nanoparticle size and weaker synergistic effect than PtBi/CNT were found in the samples of Pt-Bi/CNT (with Bi loading first and then Pt) and Bi-Pt/CNT (with Pt loading first and then Bi). Relative TEM, XPS and electrochemical results were shown in Supporting information Fig. S3 to S5. And their catalytic performance was shown in Fig. 8. PtBi/CNT presents higher conversion and selectivity than both Pt-Bi/CNT and Bi-Pt/CNT. The catalytic performance of PtBi/CNT with 5% wt. Pt loading and various Bi/Pt ratios were shown in Fig. 8. As the Bi/Pt molar ratio increases from 0 to 0.75, benzyl alcohol conversion remarkably increase from 16.5% to 55%, and reach the plateau after that till the Bi/Pt ratio increases to 1.0. The benzyl alcohol conversion slightly decreases when further increasing the ratio from 1.0 to 2.5. The selectivity towards benzaldehyde increases to the maximum as the Bi/Pt ratio increases from 0 (87.1%) to 0.1 (93.2%), and then slightly decreases when the Bi/Pt ratio further increases from 0.1 to 0.75 (90.5%), and finally reaches a plateau of about 90% when further increasing the ratio from 0.75 to 2.5. Interestingly, when adding a small amount of Bi (Bi/Pt = 0.01), no significant change of conversion can be observed. Nevertheless, the selectivity to benzaldehyde remarkably increases, which is according with the electrochemical measurement results in Fig. 6b that Bi can sensitively suppress the oxidation of benzaldehyde to benzoic

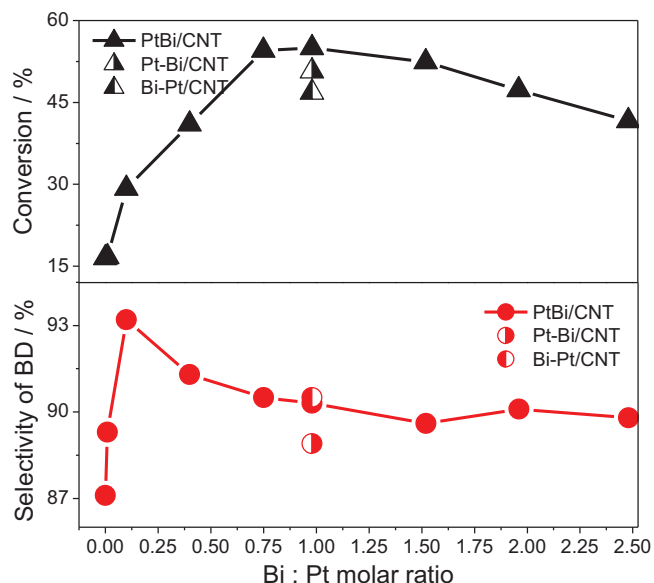


Fig. 8. Effect of loading sequence and Bi/Pt molar ratio for PtBi catalysts (all with 5% wt. Pt) in the aerobic oxidation of benzyl alcohol (conditions: benzyl alcohol 3 mmol, deionized water 15 mL, catalyst 12 mg (0.003 mmol Pt), 348 K, 3 h, O₂ flow rate 25 mL/min, carbon balance > 99.5%).

acid. The conversion of benzyl alcohol is slightly decreasing with increasing the Bi/Pt ratio from 1.0 to 2.5, probably due to the coverage of Pt sites by too much Bi. The highest benzaldehyde yield is achieved at Bi/Pt molar ratio of 0.75, which should be determined as the optimum Bi/Pt molar ratio for PtBi/CNT catalyst.

Fig. 9 shows the time course duration of PtBi/CNT and Pt/CNT in the benzyl alcohol aerobic oxidation. The conversion over PtBi/CNT is remarkably improved compared to Pt/CNT as the reaction time proceeds. After 15 min of reaction duration, the conversion of PtBi/CNT is nearly two times as that of Pt/CNT. As the reaction time increases to 3 h, almost 6 times higher conversion is observed. The initial selectivities towards benzaldehyde for both catalysts are 100%. As the reaction time reaching to 3 h, the selectivity decreases to 87% for Pt/CNT and 90.3% for PtBi/CNT.

The effects of reaction conditions such as gas atmosphere, solvent and similar alcohol substrates were also studied and the

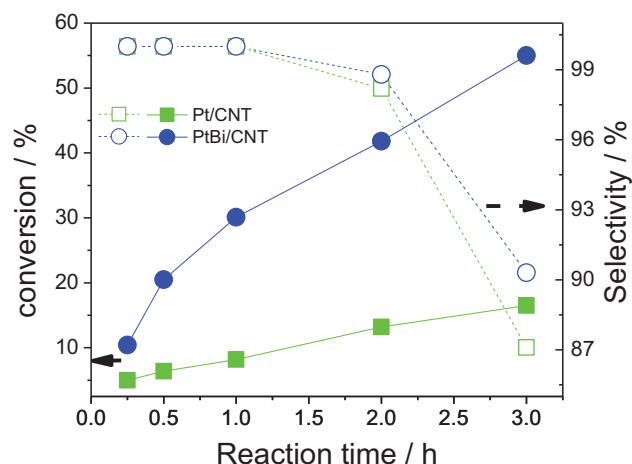


Fig. 9. Kinetic curves for PtBi/CNT and Pt/CNT in aerobic oxidation of benzyl alcohol (conditions: benzyl alcohol 3 mmol, deionized water 15 mL, 348 K, 0.25–3 h, O₂ flow rate 25 mL/min, carbon balance > 99.5%).

results are shown in Fig. 10. Aerobic and anaerobic conditions are attempted to test the catalyst performance as shown in Fig. 10a. Under argon anaerobic condition, both PtBi/CNT and Pt/CNT catalysts show nearly no activity. Both catalysts show remarkably improved activities under air and the conversion over PtBi/CNT is nearly 4 times higher than that of Pt/CNT. Activities of both catalysts are further promoted in the presence of pure oxygen, and the conversion over PtBi/CNT is about 3 times as that of Pt/CNT. Toluene, cyclohexane and water are employed as different solvents in the reactions and the results are shown in Fig. 10b. Pt/CNT shows extremely poor conversion in non-polar solution, such as toluene and cyclohexane, and polar solvent such as water favors the catalytic activity of Pt/CNT. Compared to Pt/CNT, PtBi/CNT shows promoted conversion in both of non-polar and polar solutions, and the best performance occurs in the water solution. For comparing the performance of PtBi/CNT to Pt-Bi/Al₂O₃ catalyst reported by Baiker et al. [29], similar experiment conditions were followed, and the conversion of PtBi/CNT in water is almost as high as that of Pt-Bi/Al₂O₃ in cyclohexane (as listed in Table S2). That may be due to the good hydrophilicity of the strong acid treated CNT. 4-nitrobenzyl alcohol and 4-methylbenzyl alcohol are attempted

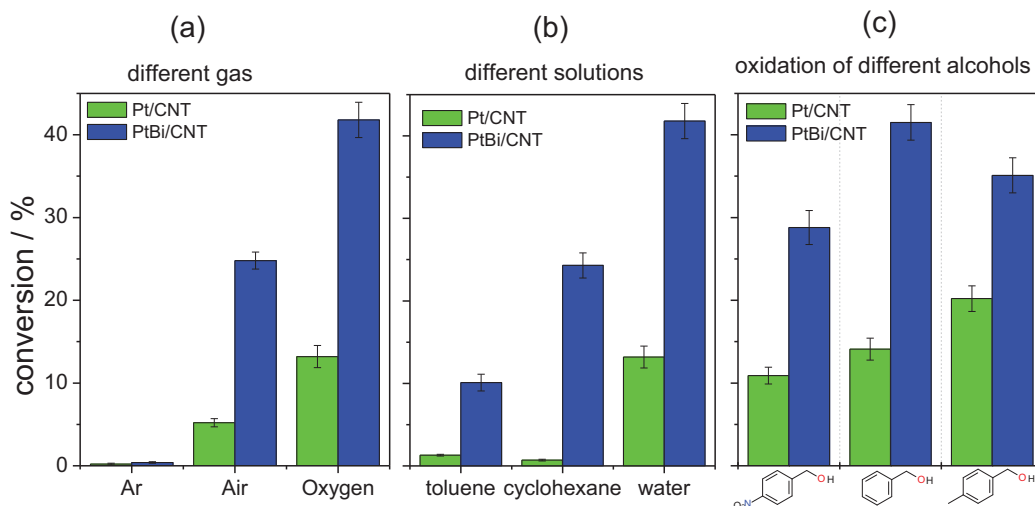


Fig. 10. Activities of Pt/CNT and PtBi/CNT in the oxidation of alcohol (conditions: (a) benzyl alcohol 3 mmol, deionized water 15 mL, catalyst 12 mg (0.003 mmol Pt), gas flow rate 25 mL/min, 348 K, 2 h; (b) benzyl alcohol 3 mmol, solution 15 mL, catalyst 12 mg (0.003 mmol Pt), O₂ flow rate 25 mL/min, 348 K, 2 h; (c) alcohol 1 mmol, deionized water 50 mL, catalyst 4 mg (0.001 mmol Pt), O₂ flow rate 25 mL/min, 348 K, 2 h; all carbon balance > 99.5%).

to examine the substrate scope of the catalysts for alcohol oxidation. 4-methylbenzyl alcohol shows a higher conversion, while 4-nitrobenzyl alcohol showing a lower conversion over Pt/CNT catalyst compared to benzyl alcohol, suggesting that Pt catalyst shows higher catalytic activity for substituted aromatic alcohols containing $-CH_3$ than those containing $-NO_2$ [59]. Compared to Pt/CNT, PtBi/CNT catalyst shows improved catalytic activity to all the substrates tested in this study. Furthermore, PtBi/CNT also affords higher catalytic activity in aromatic alcohol containing electron-donating group than that containing electro-withdrawing group. Nonetheless, the catalytic activity of benzyl alcohol is no longer moderate but the best compared to both 4-methylbenzyl alcohol and 4-nitrobenzyl alcohol, implying that the electronic effect or atomic arrangements for Pt active sites are significantly changed by adding a p-electron metal promoter of Bi [36]. Summarily, one-step preparing PtBi/CNT with near 0.75 Bi/Pt ratio presents best catalytic activity on aqueous aerobic oxidation of benzyl alcohol, and the promoted effect of Bi exists in long time reaction and various reaction conditions.

4. Conclusions

In this study, uniform Bi promoted Pt nanoparticle catalyst was successfully prepared onto CNT by a one-step microwave-assisted polyol reduction procedure, and strong synergic effect of Bi and Pt was detected in as prepared PtBi/CNT, and excellent catalytic activity and stability were also acquired in aqueous aerobic oxidation of benzyl alcohol. The synergic effect of Bi and Pt in PtBi/CNT was proved to achieve high catalytic activity by effectively promoting the activation of molecular oxygen and benzyl alcohol substrate; and obtain high selectivity by suppressing the formation of by-products; and maintain high stability by protecting Pt active sites from oxidizing. All these factors make PtBi/CNT to be a green and effective catalyst for selective oxidation of alcohols.

Acknowledgement

Y. Yang et al. acknowledge the financial support from the National Research Foundation (NRF), Prime Minister's Office, Singapore under its Campus for Research Excellence and Technological Enterprise (CREATE) program and AcRF Tier 1 grant (RG129/14), Ministry of Education, Singapore.

Appendix A. Supplementary data

Supplementary data associated with this article can be found, in the online version, at <http://dx.doi.org/10.1016/j.apcatb.2015.07.048>

References

- [1] M. Besson, P. Gallezot, *Catal. Today* 57 (2000) 127–141.
- [2] C. Keresszegi, J.D. Grunwaldt, T. Mallat, A. Baiker, *Chem. commun.* (2003) 2304–2305.
- [3] D. Ferri, A. Baiker, *Top. Catal.* 52 (2009) 1323–1333.
- [4] C. Mondelli, D. Ferri, J. Grunwaldt, F. Krumeich, S. Mangold, R. Psaro, A. Baiker, *J. Catal.* 252 (2007) 77–87.
- [5] C. Keresszegi, J.D. Grunwaldt, T. Mallat, A. Baiker, *J. Catal.* 222 (2004) 268–280.
- [6] C. Mondelli, J.D. Grunwaldt, D. Ferri, A. Baiker, *Phys. Chem. Chem. Phys.* 12 (2010) 5307–5316.
- [7] A. Zalaneeva, A. Serov, M. Padilla, U. Martinez, K. Artyushkova, S. Baranton, C. Coutanceau, P.B. Atanassov, *J. Am. Chem. Soc.* 136 (2014) 3937–3945.
- [8] R.F. Nie, D. Liang, L. Shen, J. Gao, P. Chen, Z. Hou, *Appl. Catal. B: Environ.* 127 (2012) 212–220.
- [9] Y. Kwon, Y. Birdja, I. Spanos, P. Rodriguez, M.T.M. Koper, *ACS Catal.* 2 (2012) 759–764.
- [10] T. Mallat, A. Baiker, *Appl. Catal.* 79 (1991) 41–58.
- [11] H. Kimura, K. Tsuto, T. Wakisaka, Y. Kazumi, Y. Inaya, *Appl. Catal. A: Gen.* 96 (1993) 217–228.
- [12] H. Kimura, *Appl. Catal. A: Gen.* 105 (1993) 147–158.
- [13] R. Garcia, M. Besson, P. Gallezot, *Appl. Catal. A: Gen.* 127 (1995) 165–176.
- [14] M. Besson, F. Lahmer, P. Gallezot, P. Fuertes, G. Fleche, *J. Catal.* 152 (1995) 116–121.
- [15] M. Wenkin, R. Touillaux, P. Ruiz, B. Delmon, M. Devillers, *Appl. Catal. A: Gen.* 148 (1996) 181–199.
- [16] F. Alard, P. Ruiz, B. Delmon, M. Devillers, *Appl. Catal. A: Gen.* 215 (2001) 125–136.
- [17] T. Mallat, C. Bronnimann, A. Baiker, *J. Mol. Catal. A: Chem.* 117 (1997) 425–438.
- [18] A.B. Crozon, M. Besson, P. Gallezot, *New J. Chem.* 22 (1998) 269–273.
- [19] Y. Zhou, S.X. Wang, B.J. Ding, Z.M. Yang, *J. Sol-Gel. Sci. Technol.* 47 (2008) 182–186.
- [20] T. Lu, Z. Du, J. Liu, H. Ma, J. Xu, *Green Chem.* 15 (2013) 2215–2221.
- [21] T. Mallat, Z. Bodnar, P. Hug, A. Baiker, *J. Catal.* 153 (1995) 131–143.
- [22] G. Jenzer, D. Sœur, T. Mallat, A. Baiker, *Chem. Commun* (2000) 2247–2248.
- [23] C. Keresszegi, J.D. Grunwaldt, T. Mallat, A. Baiker, *Chem. Commun.* (2003) 2304–2305.
- [24] C. Keresszegi, T. Mallat, J.D. Grunwaldt, A. Baiker, *J. Catal.* 225 (2004) 138–146.
- [25] C. Keresszegi, J.D. Grunwaldt, T. Mallat, A. Baiker, *J. Catal.* 222 (2004) 268–280.
- [26] C. Mondelli, D. Ferri, J.D. Grunwaldt, F. Krumeich, S. Mangold, R. Psaro, A. Baiker, *J. Catal.* 252 (2007) 77–87.
- [27] D. Ferri, A. Baiker, *Top. Catal.* 52 (2009) 1323–1333.
- [28] S. Marx, A. Baiker, *J. Phys. Chem. C* 113 (2009) 6191–6201.
- [29] C. Mondelli, J.D. Grunwaldt, D. Ferri, A. Baiker, *Phys. Chem. Chem. Phys.* 12 (2010) 5307–5316.
- [30] D.I. Enache, J.K. Edwards, P. Landon, B. Solsona-Espriu, A.F. Carley, A.A. Herzing, M. Watanabe, C.J. Kiely, D.W. Knight, G.J. Hutchings, *Science* 311 (2006) 362–365.
- [31] P.C.C. Smits, B.F.M. Kuster, K. Vanderwiele, H.S. Vanderbaan, *Appl. Catal.* 33 (1987) 83–96.
- [32] A. Abbadi, K.F. Gotlieb, J.B.M. Meiberg, H. VanBekkum, *Appl. Catal. A: Gen.* 156 (1997) 105–115.
- [33] P. Fordham, M. Besson, P. Gallezot, *Catal. Lett.* 46 (1997) 195–199.
- [34] A. Villa, D. Wang, G.M. Veith, L. Prati, *J. Catal.* 292 (2012) 73–80.
- [35] M. Wenkin, P. Ruiz, B. Delmon, M. Devillers, *J. Mol. Catal. A: Chem.* 180 (2002) 141–159.
- [36] T. Mallat, Z. Bodnar, A. Baiker, O. Greis, H. Strubig, A. Reller, *J. Catal.* 142 (1993) 237–253.
- [37] H. Hayashi, S. Sugiyama, N. Shigemoto, K. Miyaura, S. Tsujino, K. Kawashiro, S. Uemura, *Catal. Lett.* 19 (1993) 369–373.
- [38] A. Abbadi, H. VanBekkum, *Appl. Catal. A: Gen.* 124 (1995) 409–417.
- [39] A. Abbadi, H. VanBekkum, *J. Mol. Catal. A: Chem.* 97 (1995) 111–118.
- [40] H. Kimura, A. Kimura, I. Kokubo, T. Wakisaka, Y. Mitsuda, *Appl. Catal. A: Gen.* 95 (1993) 143–169.
- [41] J. Yang, Y.J. Guan, T. Verhoeven, R. van Santen, C. Li, E.J.M. Hensen, *Green Chem.* 11 (2009) 322–325.
- [42] W. Hu, D. Knight, B. Lowry, A. Varma, *Ind. Eng. Chem. Res.* 49 (2010) 10876–10882.
- [43] N. Woerz, A. Brandner, P. Claus, *J. Phys. Chem. C* 114 (2010) 1164–1172.
- [44] H.A. Rass, N. Essayem, M. Besson, *Green Chem.* 8 (2013) 2240–2251.
- [45] I.D. Rosca, F. Watari, M. Uo, T. Akaska, *Carbon* 43 (2005) 3124–3131.
- [46] J.H. Bitter, A.J. Plomp, D.M.P. van Asten, A.M.J. van der Eerden, P. Maki-Arvela, D.Y. Murzin, K.P. de Jong, *J. Catal.* 263 (2009) 146–154.
- [47] Y.Y. Huang, J.D. Cai, Y.L. Guo, *Appl. Catal. B: Environ.* 129 (2013) 549–555.
- [48] Y.M. Liang, H.M. Zhang, H.X. Zhong, X.B. Zhu, Z.Q. Tian, D.Y. Xu, B.L. Yi, *J. Catal.* 238 (2006) 468–476.
- [49] J.D. Grunwaldt, M.D. Wildberger, T. Mallat, A. Baiker, *J. Catal.* 177 (1998) 53–59.
- [50] N. Myung, S. Ham, S. Choi, W.G. Kim, Y.J. Jeon, K.J. Paeng, W. Chanmanee, N.R. de Tacconi, K. Rajeshwar, *J. Phys. Chem. C* 115 (2011) 7793–7800.
- [51] A. Pozio, M. De Francesco, A. Cemmi, F. Cardellini, L. Giorgi, *J. Power Sources* 105 (2002) 13–19.
- [52] Y. Huang, J. Cai, Y. Guo, *Appl. Catal. B: Environ.* 129 (2013) 549–555.
- [53] A. Zalaneeva, S. Baranton, C. Coutanceau, *Electrochim. Commun.* 34 (2013) 335–338.
- [54] L. Demarconnay, S. Brimaud, C. Coutanceau, J.M. Leger, *J. Electroanal. Chem.* 601 (2007) 169–180.
- [55] L. Demarconnay, C. Coutanceau, J.M. Leger, *Electrochim. Acta* 53 (2008) 3232–3241.
- [56] M. Simoes, S. Baranton, C. Coutanceau, *Appl. Catal. B: Environ.* 110 (2011) 40–49.
- [57] Y.M. Liang, H.M. Zhang, H.X. Zhong, X.B. Zhu, Z.Q. Tian, D.Y. Xu, B.L. Yi, *J. Catal.* 260 (2008), 392–392.
- [58] B.N. Zope, D.D. Hibbitts, M. Neurock, R.J. Davis, *Science* 330 (2010) 74–78.
- [59] Y.T. Chen, Z. Guo, T. Chen, Y.H. Yang, *J. Catal.* 275 (2010) 11–24.